

See discussions, stats, and author profiles for this publication at: <https://www.researchgate.net/publication/261436611>

# Layers of Polyaniline Nanotubes Deposited by Langmuir–Blodgett Method

ARTICLE *in* THE JOURNAL OF PHYSICAL CHEMISTRY C · MAY 2012

Impact Factor: 4.77 · DOI: 10.1021/jp302040v

---

CITATIONS

6

---

READS

25

## 3 AUTHORS:



[Barbara Pałys](#)

University of Warsaw

61 PUBLICATIONS 1,132 CITATIONS

[SEE PROFILE](#)



[Piotr Olejnik](#)

University of Warsaw

5 PUBLICATIONS 38 CITATIONS

[SEE PROFILE](#)



[Marianna Gniadek](#)

University of Warsaw

18 PUBLICATIONS 108 CITATIONS

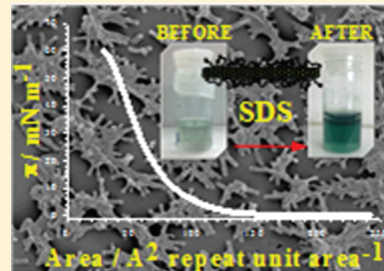
[SEE PROFILE](#)

# Layers of Polyaniline Nanotubes Deposited by Langmuir–Blodgett Method

Piotr Olejnik, Marianna Gniadek, and Barbara Palys\*

Department of Chemistry, University of Warsaw, Pasteura 1, 02-093 Warsaw, Poland

**ABSTRACT:** The Langmuir–Blodgett (LB) method has long been used for the preparation of ultrathin films, offering the unique control over the film thickness and the molecular orientation. Here, we report on the deposition and the characterization of LB layers of polyaniline (PANI) nanotubes on solid supports. Stable suspension of the nanotubes in chloroform was obtained by adding sodium dodecyl sulfate (SDS). The nanotubes to SDS ratio is important for the stability of the suspension. Langmuir films were spread at the water/air interface and transferred on gold or ITO glass substrate. The electroactivity of obtained films was investigated using cyclic voltammetry. The degree of assembly of the PANI nanotubes in thin films was characterized by optical microscopy and scanning electron microscopy (SEM). To evaluate the molecular structure and the PANI oxidation state, UV–vis and Raman mapping were used. The PANI nanotube films on the gold support are electroactive with cyclic voltammetry responses closely resembling typical PANI layers. Raman maps reveal that the spatial distributions of SDS and PANI bands are identical, suggesting that only detergent molecules bond to nanotubes are transferred on the support.



## 1. INTRODUCTION

The nanostructured conducting polymers have received much interest due to their high surface to volume ratio, and high surface free energy, resulting in electronic and physical properties that are interesting for biosensing applications.<sup>1–4</sup> Biologically important molecules can be easily incorporated into the conducting polymer nanotubes either during or after the polymer synthesis. The modification can be realized by a physical entrapment enforced by the electrostatic interaction with the polymer charge carriers. Biomolecules can be also introduced by adsorption or chemical bonding to the polymer functional groups. Polymeric conductivity can be controlled by the oxidation state, pH, and the kind of doping ion. Such flexibility opens numerous possibilities for the application in biosensors field. Because of the alignment of the polymer chains and strong intermolecular interactions, conducting polymer nanotubes reveal superior conductivity as compared to the bulk polymer layers.<sup>5–7</sup> Polymer chains forming nanotube walls might attain a single conformation depending on the synthesis conditions, which in turn might influence their cyclic voltammetry responses.<sup>8–10</sup>

The most effective and simple method to obtain polymer nanotubes is template synthesis.<sup>11–14</sup> The template method enables the control over the nanotube size, which in consequence affects the properties of nanotubes. Processability and storage of conducting polymer nanotubes remain still unsolved issues. Because of the strong interchain interactions, conducting polymers are hardly soluble in common organic solvents. Poor solubility is beneficial for the stability of the polymeric nanostructures, but it complicates the deposition on conducting surfaces by casting method. The solubility of the nanostructures in a volatile solvent, not miscible with water, is also a prerequisite to obtain the stable Langmuir film. In

current study, the surfactant dodecylbenzenesulfonic acid (SDS) has been used to obtain the suspension of PANI nanotubes in chloroform. The effect of SDS to PANI proportion is considered.

Among the many methods of layer assembly on conductive support, the LB technique gains increasing interest because of its simplicity, low cost, and unique ability to control the film ordering by mechanical forces at the water–air interface. The thickness of the film could be controlled by the alternate monomolecular layer by layer transfer onto the solid support. The LB method is typically applied to amphiphilic substances, detergents and lipids,<sup>15</sup> although extensive research is carried out on Langmuir films of polymer, liquid crystals, proteins, DNA, carbon nanotubes, and inorganic nanostructures. A comprehensive review on the unusual Langmuir films can be found in refs 16–19. The LB method offers the unique ability to study the conformation of peptides and other macromolecules upon surface pressure changes. Ariga et al. have demonstrated the molecular recognition pattern of cyclophane steroid complexes can be controlled by motion of host molecules on the air–water interface.<sup>20,21</sup> The combination of LB and spectroscopic methods has been applied for study of the protein conformation in Langmuir films<sup>22–24</sup> and hybridization of DNA on phospholipid layers.<sup>25</sup>

LB technique has been also applied for deposition of conducting polymer films to obtain highly ordered structures.<sup>26–33</sup> Among others, Swager et al.<sup>33</sup> have demonstrated that the conformation of the poly(*p*-phenyleneethynylene)s can be controlled by amphiphilic substituents. The conformation, in

Received: March 1, 2012

Revised: April 12, 2012

Published: April 18, 2012



ACS Publications

© 2012 American Chemical Society

10424

dx.doi.org/10.1021/jp302040v | J. Phys. Chem. C 2012, 116, 10424–10429

turn, influences the UV-vis and fluorescence spectra of the polymer. Application of LB creates new possibilities for microelectronic devices construction.

Conducting polymer nanotubes do not resemble typical surface active compounds, because they do not have the hydrophilic head and hydrophobic tail. Their assembly on the air–water interface would resemble inorganic and carbon nanotubes described by the “logs on the river” concept<sup>17,34,35</sup> involving ordering of the nanotubes parallel to the moving barriers. Similarly to carbon nanotubes, conducting polymer nanostructures undergo heavy aggregation in the solution phase due to strong  $\pi$ – $\pi$  interactions. In consequence, the nanotube films deposited by solution casting or spin-coating techniques consist of disordered and often bent structures. The application of LB enables deposition of aligned nanotubes on solid supports.

In this Article, we test the applicability of the LB method to the deposition thin layers of PANI nanotubes on a solid support. To our knowledge, the LB method was not used for conducting polymer nanotubes layers.

Numerous applications of PANI include gas sensors,<sup>36–38</sup> vitamin C sensor,<sup>39</sup> pH indicators,<sup>40</sup> bacteria detection,<sup>41</sup> and enzyme support.<sup>42,43</sup> The object of this study is to form ordered conducting surfaces characterized by large surface area, through the deposition of PANI nanotubes layers using LB technique. The nanotubes are characterized by larger surface area than polymer thin films; therefore, using PANI nanotubes instead of PANI films will be beneficial for both direct sensing applications and use of PANI as the enzyme support.

## 2. EXPERIMENTAL SECTION

**2.1. Chemicals.** Aniline monomer and sulfuric acid 95–97% were purchased from POCh. Ammonium persulfate 98% ( $(\text{NH}_4)_2\text{S}_2\text{O}_8$ ), sodium dodecylsulfate, sodium salt 98% (SDS), and dodecylbenzenesulfonic acid 98% were purchased from Sigma Aldrich. Chloroform solvent was obtained from Chempur. All reagents (p.a. grade) were used without further purification. All solutions were prepared with water purified by a Milli-Q system, with resistivity of 18.2 M $\Omega$  and pH 7.

**2.2. Measurements.** Polyaniline nanotubes layers were deposited using NIMA 611 trough. The formation of LB films was confirmed first by analyzing the transfer ratio. The films deposited on the ITO support were studied using UV-vis spectroscopy with Lambda 12 from Perkin-Elmer. PANI nanotubes on ITO and gold supports were studied by Raman spectroscopy (HR LABRAM 800 from Horiba Jobin Yvon with 632.8 nm He–Ne excitation line). Electrochemical measurements were made using a potentiostat PGSTAT 20 from AUTOLAB Eco Chemie and were carried out in a trielectrode system in which the working electrode was a plate of gold, a reference electrode, silver/silver chloride electrode in 3 M NaCl (Ag/AgCl), and an auxiliary electrode, platinum net. To observe the morphology of the obtained layers, the optical microscope Nikon H600L and the field emission scanning electron microscope (SEM) ZEISS were used.

**2.3. Synthesis of PANI Nanotubes.** The synthesis of PANI nanotubes was achieved by the template method. The Whatman Nuclepore polycarbonate membranes were used as templates. The pore diameters were either 100 or 400 nm. The synthesis was carried out in 1 M sulfuric acid medium by the chemical oxidation of the monomer using ammonium persulfate as oxidant.

In a typical experiment, PC membrane was soaked in 5 mL of 0.3 M aniline acidic solution for 30 min and after that mixed with 5 mL of 0.3 M  $(\text{NH}_4)_2\text{S}_2\text{O}_8$  in 1 M sulfuric acid solution. The reaction vessel was kept at low temperature ( $\sim 4^\circ\text{C}$ ). The typical reaction time was about 3 h. After that, the membrane was removed, rinsed with distilled water, and dried.

**2.4. Template Removal.** To separate PANI nanotubes, polycarbonate membrane was removed by dissolving in chloroform. To get rid of the dissolved polycarbonate, the chloroform solution was moved into an extractor and shaken with 1 M  $\text{H}_2\text{SO}_4$ . PANI nanotubes created a green layer at the interface between chloroform and sulfuric acid. The extraction process was repeated 10 times, and the polycarbonate was totally eluted. The water layer has been removed by the Pasteur pipet. The chloroform fraction was poured into the glass flask, and some chloroform was added to obtain 4 mL of the solution (4 mL per one filtration membrane). The purity and undisturbed morphology of PANI nanotubes has been verified by optical microscopy (Figure 1). For this purpose, nanotubes were placed on a gold plate using a Pasteur pipet. The picture has been registered using the reflectance mode.

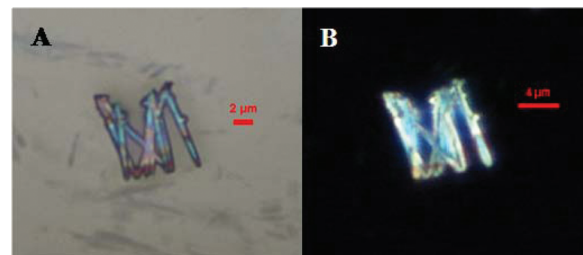


**Figure 1.** Optical microscopy images of PANI nanotubes with a diameter of 400 nm after polycarbonate removing: in light field (A) and dark field (B) modes.

## 3. RESULTS AND DISCUSSION

**3.1. Chloroform Suspension of PANI Nanotubes.** To obtain the Langmuir films on the water surface, PANI nanotubes had to be dispersed in a solvent not miscible with water. Chloroform was chosen because of the short time of evaporation. Furthermore, the PANI nanotube integrity would not be affected, because PANI is not soluble in chloroform. The PANI nanotubes reveal a tendency to aggregate in the chloroform solutions. Even upon applying the ultrasonic bath, the visible green clumps are formed. Several surface active agents including sodium dodecylsulfate (SDS), 4-dodecylbenzenesulfonic acid, Tween 85, Tween 65, Span 60, and Span 65 were tested as possible emulsifiers. Only SDS brought acceptable effects. The homogeneous green, colloid solution has been obtained, which is shown in Figure 2.

The optimal amount of SDS to obtain the solution of nanotubes is 100  $\mu\text{L}$  of the 0.25 M aqueous SDS solution per 4 mL of chloroform solution of nanotubes. The surfactant does not affect the nanotubes morphology. PANI nanotubes remain straight. Their length reaches a few micrometers, similarly to those shown in Figure 1. A larger amount of SDS solution ( $>100 \mu\text{L}$ ) gives a green homogeneous suspension as well, but the microscope images reveal bent or damaged PANI nanotubes. If solution, containing a high amount of SDS, is spread onto the water surface, the nanotubes sink in the water.

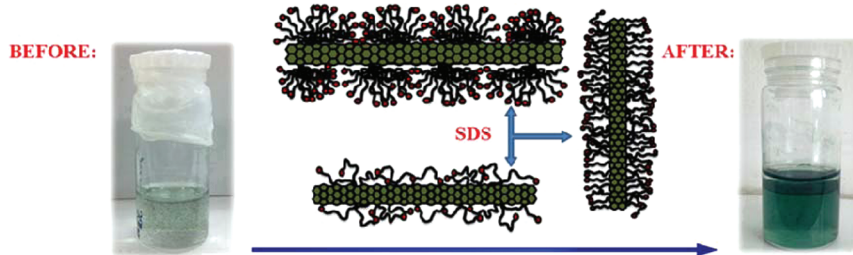


**Figure 2.** SDS ( $100 \mu\text{L}$  of  $0.25 \text{ M}$  aq solution) influence on aggregation degree of PANI nanotubes in chloroform solution (4 mL).

The optimal quantity of SDS is identical for PANI nanotubes of 100 and 400 nm diameter.

The distinguishing feature of SDS among other tested surfactants is high polarity combined with good solubility in chloroform. SDS molecules interact probably with charged sites on the PANI nanotube surface. The surfactant molecules sticking to nanotubes might organize in different ways depending on the concentration of the detergent and the concentration on PANI nanotubes as illustrated in Figure 2. A small number of SDS molecules is probably sufficient to render the solubility in chloroform. Too many SDS molecules increase the nanotube weight. In consequence, nanotubes are too heavy to remain on the water surface. A large amount of SDS attached to PANI might also make nanotubes brittle.

### 3.2. Creation and Immobilization of PANI Nanotube LB Layers.

Figure 3 shows the typical surface pressure—

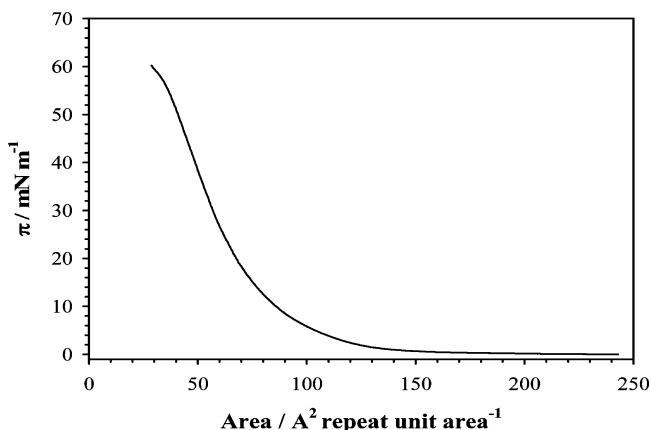
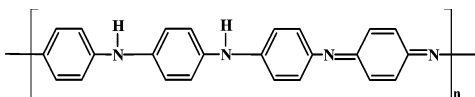


**Figure 3.** Surface pressure as a function of molecular area per PANI repeat unit for a PANI nanotubes/SDS ( $100 \mu\text{L}$ ) assembly at the water/air interface.

molecular area ( $\pi$ - $A$ ) isotherm of the PANI nanotubes monolayer on water subphase at pH value equal to 6.3. The molecular area was calculated for a PANI repeat unit (Scheme 1) with a total molecular weight equal to  $362 \text{ g mol}^{-1}$ .

The shape of the isotherm does not depend on the nanotube diameter; therefore, only results for the 100 nm are presented in Figure 3. The flat segment of the isotherm corresponds to the gas phase. The flat part in which no change in surface

### Scheme 1. Repeat Unit of PANI in the Conductive Form, $362 \text{ g mol}^{-1}$



pressure is observed indicates that the PANI nanotubes are widely spread over the water surface and do not interact with each other. The pressure starts rising at ca.  $130 \text{ Å}^2 \text{ molecule}^{-1}$ . The slow increase in pressure up to  $20 \text{ mN m}^{-1}$  could be attributed to the liquid state of the layer. A further steep increase suggests the formation of the stable solid layer. The formation of the stable layer can be further supported by quite high collapse pressure equal to  $62 \text{ mN m}^{-1}$ .

The average area for the PANI repeat unit estimated by the extrapolation of the linear part of the isotherm is equal to  $80 \text{ Å}^2$ . Similar repeat unit area values have been reported for PANI doped with large amphiphilic dopants.<sup>44,45</sup>

Studies of Langmuir films of PANI and related polymers revealed that the mean area per polymer repeat value depends on the subphase pH, the spreading solvents, and the kind of doping anion. Independently of the dopant, Langmuir isotherms of PANI revealed parallel or tilted orientation of the polymer with respect to the water surface. The area values reported for PANI and poly alkoxyanilines doped with small inorganic anions<sup>31,32,46</sup> are of the order of  $20 \text{ Å}^2$  for the acidic subphase. The increase of the pH value causes an increase of the mean molecular area up to  $60 \text{ Å}^2$ . The higher molecular area has been attributed to the less ordered Langmuir film. It has been also reported that the large amphiphilic dopant causes a large increase of the repeat unit area, although formation of ordered polymer films has been shown.<sup>44,45</sup>

The solubility of SDS in water affects the surface pressure values, which contributes possibly to the increase of the repeat unit area obtained in this study.

To obtain repeatable Langmuir–Blodgett films on a solid support, the stable conditions for the layer on water have to be found. To determine the stability of PANI nanotubes films on the water–air interface, the dependence of the area changes on time at constant pressure was studied. Typical results are presented in Figure 4A. The experiment lasted about 15 h and was conducted at a constant pressure equal to  $25 \text{ mN m}^{-1}$ . The chosen pressure value corresponds to the solid state part of the Langmuir isotherm.

As illustrated in Figure 4A, the molecular area reaches a stable value after 40 min. After this time, the surface virtually does not change, and the layer is ready to transfer onto the solid support.

PANI nanotubes layer formed by the Langmuir–Blodgett method were deposited on the solid surface (gold or ITO) by emerging the gold substrate perpendicularly to the interface at a speed of  $10 \text{ mm min}^{-1}$  and at the controlled surface pressure value equal to  $25 \text{ mN m}^{-1}$ . The typical transfer ratio values for both gold and ITO substrates were equal to 0.8. The horizontal Langmuir–Schaefer transfer mode revealed worse transfer ratios, less than 0.5. The reason for better transfer ratio values

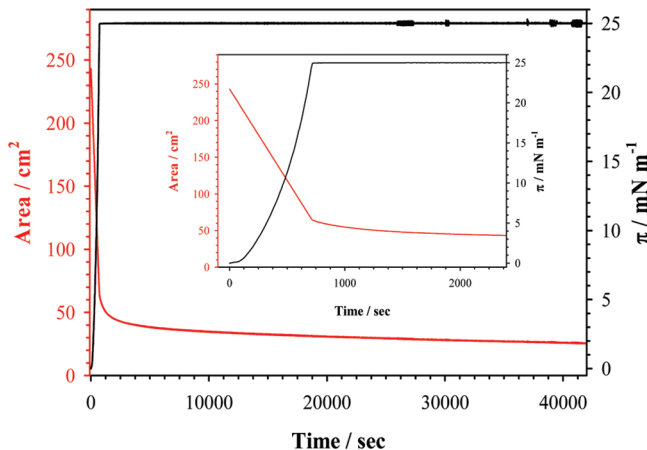


**Figure 4.** The dependence of the surface changes from time at a constant pressure of  $25 \text{ mN m}^{-1}$  for PANI nanotubes.

for the LB deposition mode is probably the good control of the surface pressure ensuring the stability of the Langmuir film.

Figure 5 shows a representative SEM image of PANI nanotubes layer transferred on the gold support. As is visible in

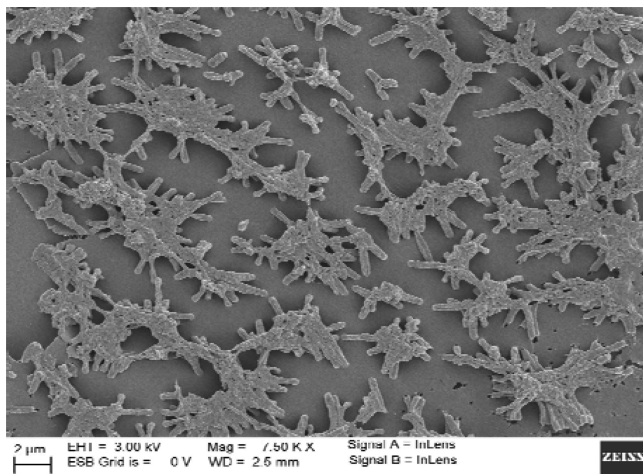


**Figure 5.** SEM image of PANI nanotubes with a diameter of 100 nm transferred on a gold support by the LB method.

Figure 5, PANI nanotubes are clearly grouped in bundles, although the dispersion of PANI nanotubes in chloroform was stable for several days. The possible reason for the aggregation of nanotubes at the water/air interface might be gradual dissolution of SDS in the water subphase during the layer stabilization. Too low of a surface concentration of SDS promotes the interaction between nanotubes at the water/air interface. The PANI nanotubes diameter and length are preserved on the surface.

**3.3. Visible Absorption Spectroscopy.** The typical visible absorption spectrum of a layer of PANI nanotubes with a diameter 400 nm with the addition of  $100 \mu\text{L}$  of SDS deposited on ITO glass is shown in Figure 6.

The spectrum indicates the presence of PANI in the conductive form. Polaronic species contributing to the PANI conductivity are visualized by the  $425 \text{ nm}$  band.<sup>47,48</sup> Another spectral signature of polarons is expected at  $880 \text{ nm}$ . In the spectrum presented in Figure 6, this band overlaps with the intense band ranging from  $600$  to  $850 \text{ nm}$ , signifying the

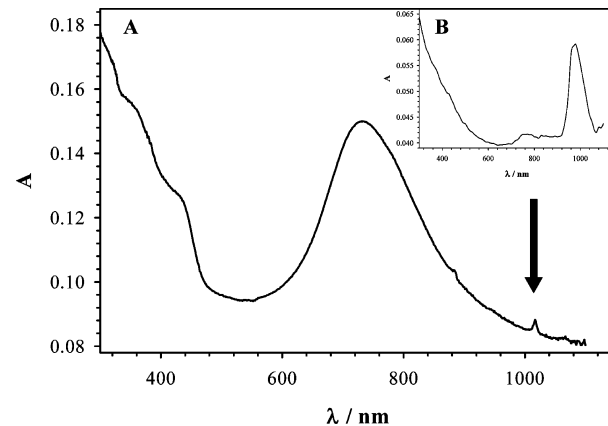


**Figure 6.** Visible absorption spectra of (A) PANI nanotubes layer with a diameter of 400 nm and addition of  $100 \mu\text{L}$  of SDS; the pure ITO glass was used to record the background; and (B)  $0.25 \text{ M}$  SDS; the cell filled with water was used to record the background.

presence of bipolarons and possibly quinoid structures in PANI nanotubes. The presence of quinoid structures indicates that PANI is partially deprotonated in results of the interaction with the subphase.<sup>31</sup>

To evaluate the possible contribution of SDS to the layer absorption, the spectrum of SDS solution has been recorded (Figure 6B). The signal appearing at a wavelength  $\sim 1020 \text{ nm}$  ( $9804 \text{ cm}^{-1}$ ) is associated with the presence of SDS. The wavelength value corresponds to the triple frequency of the O–H stretching mode. The contribution of water to the concerned band is rather improbable, because water was used to record the background spectrum; therefore, we suppose that the  $1020 \text{ nm}$  band corresponds to the overtone of the O–H stretching mode of the SDS carboxyl group.

In the PANI-layer spectra, the weak band appears at  $1020 \text{ nm}$ . The low intensity of the SDS band suggests that only a small amount of this compound is transferred on the ITO glass plate.

Application of UV-vis spectroscopy confirms the effectiveness of the PANI nanotubes layer transfer on the substrate and their presence on a solid support. The obtained spectra indicated the presence of polaronic charge carriers as well as deprotonated fragments of PANI nanotubes. Spectra indicated also the presence of SDS in the nanotubes film.

**3.4. Raman Spectroscopy.** Figure 7 presents typical Raman spectra of PANI nanotubes layers. The He–Ne laser line with a wavelength of  $632.8 \text{ nm}$  was used for excitation. The chosen excitation frequency falls in the range of the PANI nanotubes absorption (Figure 9). Consequently, PANI bands are resonantly enhanced. The bands due to SDS presence are difficult to discern in places, where they overlap with PANI. Only weak shoulders at  $735$  and  $600 \text{ cm}^{-1}$  could be attributed to SDS  $\text{CH}_2$  rocking and C–S stretching modes, respectively.

The main spectral features are described in the figure. The assignments are based on refs 49,50. The spectrum indicates the presence of both conductive polaronic and fully oxidized quinoid forms of PANI, staying in agreement with the visible absorption data. The presence of phenazine, which is a byproduct of the polymerization, is signified by the  $592 \text{ cm}^{-1}$  band.<sup>51</sup>

The spatial distribution of SDS in the nanotube films has been studied by Raman mapping. Dhanabalan et al. have studied PANI mixtures with cadmium stearate.<sup>45</sup> The authors

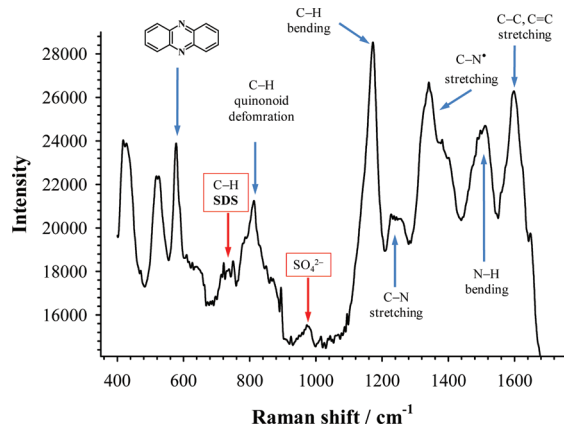


**Figure 7.** Raman spectra for PANI nanotubes (400 nm) layer (632.8 nm He-Ne excitation line).

observed an increase of the r.u. area upon increased PANI to cadmium stearate ratio. The result has been explained by poor miscibility of the polymer and surfactant, leading to the formation of stearate domains with PANI randomly oriented or stuck on the trough surface. To exclude similar domain formation by PANI nanotubes and SDS, the layers transferred on the solid support were examined by Raman mapping and are able to verify formation of SDS domains.

Figure 8 shows measurement made using the Raman mapping method. Maps were presented in different colors.

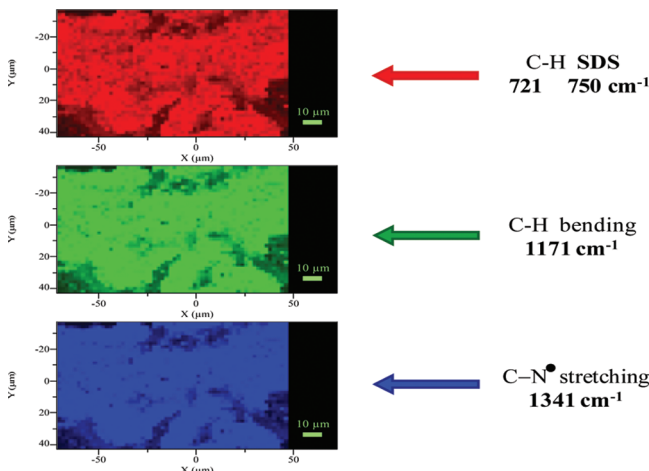


**Figure 8.** Raman maps for PANI nanotubes (400 nm) layer (632.8 nm He-Ne excitation line).

Each of them is a picture of the same sample (PANI nanotubes layer with 100  $\mu$ L of SDS on gold) but shows the intensity of other peaks.

The red map shows the distribution of signals from SDS, while green and blue show bands characteristic for PANI nanotubes. Dark spots on all maps indicate the lack of signals, while bright spots indicate their presence. On this basis, it can be seen that the layer of nanotubes is not spread evenly over the surface. Furthermore, there are definitely less SDS molecules than polyaniline nanotubes, which is satisfactory. The distribution of SDS overlaps with the distribution of PANI bands, indicating that only SDS molecules bonded to PANI are transferred on the plate.

**3.5. Cyclic Voltammetry.** The formed PANI nanotubes layer was examined electrochemically using the cyclic voltammetry technique. LB film was deposited on gold electrode. Measurement was conducted in 1 M sulfuric acid. The obtained voltammograms are shown in Figure 9.

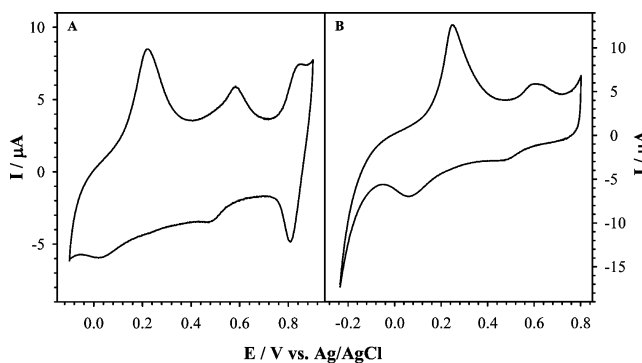


**Figure 9.** Cyclic voltammograms for PANI nanotubes (100 nm) layer with 100  $\mu$ L of 0.25 M SDS in potential ranges (a)  $-0.1 \div 0.9$  V, and (b)  $-0.3 \div 0.8$  V.

Dependencies are the same as in the case of macromolecular polyaniline. Cyclic voltammograms show two pairs of redox peaks. Despite the presence of SDS, the PANI nanotubes layer is electroactive. Previous studies of PANI nanotubes casted on electrodes showed an increase of PANI redox currents upon extension of the potential range to  $-0.2$  V vs Ag/AgCl.<sup>8</sup> The obtained voltammograms are presented in different potential ranges. We can see that regardless of what the initial potential is, redox peaks do not change, as was the case with pure PANI nanotubes. This fact is probably caused by the presence of a surfactant.

#### 4. MAIN RESULTS AND CONCLUSIONS

Experiments showed that PANI nanotubes are able to form Langmuir layers, as indicated with surface pressure, Raman spectra, and cyclic voltammetry measurements. In addition, the best degree of nanotubes disaggregation we have obtained by using 100  $\mu$ L of SDS in 4 mL of chloroform solution. SEM images illustrate that Langmuir layers are not regular, but we can immobilize them on solid substrate. UV-vis spectroscopy confirms that such formed molecular films are rich in charge carriers, polarons and bipolarons, which proves electroactivity of PANI nanotubes. PANI nanotubes deposited by the LB technique on the gold support are electroactive with cyclic voltammetry responses closely resembling typical PANI thin layers. Raman maps reveal that the spatial distributions of SDS and PANI bands are identical, suggesting that only detergent molecules bonded to nanotubes are transferred on the gold support. The nanotubes to SDS ratio is important for the stability of the suspension.

#### ■ AUTHOR INFORMATION

##### Corresponding Author

\*Tel.: +48228220211, ext. 505. E-mail: bpals@chem.uw.edu.pl

##### Notes

The authors declare no competing financial interest.

## ACKNOWLEDGMENTS

This work was supported by the Ministry of Science and Higher Education through the National Centre for Research and Development, Project No. PBR 0923/R/T02/2010/10.

## REFERENCES

- (1) Luo, X.; Morrin, A.; Killard, A. J.; Smyth, M. R. *Electroanalysis* **2006**, *18*, 319–326.
- (2) Malhorta, B. D.; Chaubey, A.; Singh, S. P. *Anal. Chim. Acta* **2006**, *578*, 59–74.
- (3) MacDiarmid, A. G. *Synth. Met.* **2001**, *40*, 2581–2590.
- (4) Wanekaya, A. K.; Chen, W.; Myung, N. V.; Mulchandani, A. *Electroanalysis* **2006**, *18*, 533–550.
- (5) Zhang, Z. M.; Deng, J. Y.; Wan, M. X. *Mater. Chem. Phys.* **2009**, *115*, 275–279.
- (6) Rahy, A.; Yang, D. J. *Mater. Lett.* **2008**, *62*, 4311–4314.
- (7) Delvaux, M.; Duchet, J.; Stavaux, P. Y.; Legras, R.; Demoustier-Champagne, S. *Synth. Met.* **2000**, *113*, 275–280.
- (8) Palys, B.; Celuch, P. *Electrochim. Acta* **2006**, *51*, 4115–4124.
- (9) Duchet, J.; Legras, R.; Demoustier-Champagne, S. *Synth. Met.* **1998**, *98*, 113–122.
- (10) Tagowska, M.; Palys, B.; Jackowska, K. *Synth. Met.* **2004**, *142*, 223–229.
- (11) Martin, C. R. *Science* **1994**, *266*, 1961–1966.
- (12) Demoustier-Champagne, S.; Duchet, J.; Legras, R. *Synth. Met.* **1999**, *101*, 20–21.
- (13) Mativetsky, J.; Datars, W. R. *Solid State Commun.* **2002**, *122*, 151–154.
- (14) Mazur, M.; Tagowska, M.; Palys, B.; Jackowska, K. *Electrochim. Commun.* **2003**, *5*, 403–407.
- (15) Czolkos, I.; Jesorka, A.; Orwar, O. *Soft Matter* **2011**, *7*, 4562–4576.
- (16) Acharya, S.; Shundo, A.; Hill, J. P.; Ariga, K. *J. Nanosci. Nanotechnol.* **2009**, *9*, 3–18.
- (17) Acharya, S.; Hill, J. P.; Ariga, K. *Adv. Mater.* **2009**, *21*, 2959–2981.
- (18) Sakakibara, K.; Hill, J. P.; Ariga, K. *Small* **2011**, *7*, 1288–1308.
- (19) Ariga, K.; Vinu, A.; Yamauchi, Y.; Ji, Q.; Hill, J. P. *Bull. Chem. Soc. Jpn.* **2012**, *85*, 1–32.
- (20) Ariga, K.; Nakanishi, T.; Hill, J. P. *Soft Matter* **2006**, *2*, 465–477.
- (21) Michinobu, T.; Schinoda, S.; Nakanishi, T.; Hill, J. P.; Fujii, K.; Player, T. N.; Tsukube, H.; Ariga, K. *J. Am. Chem. Soc.* **2006**, *128*, 14478–14479.
- (22) Yassine, W.; Milochau, A.; Buchoux, S.; Lang, J.; Desbat, B.; Oda, R. *Biochim. Biophys. Acta* **2010**, *1798*, 928–937.
- (23) Lau, T.-L.; Ambroggio, E. E.; Tew, D. J.; Cappai, R.; Masters, C. L.; Fidelio, G. D.; Barnham, K. J.; Separovic, F. *J. Mol. Biol.* **2006**, *356*, 759–770.
- (24) Rapaport, H.; Kjaer, K.; Jensen, T. R.; Leiserowitz, L.; Tirrell, D. *A. J. Am. Chem. Soc.* **2000**, *122*, 12523–12529.
- (25) Hianik, T.; Vitovic, P.; Humenik, D.; Andreev, S. Y.; Oretskaya, T. S.; Hall, E. A. H.; Vadgama, P. *Bioelectrochemistry* **2003**, *59*, 35–40.
- (26) Sarkar, N.; Ram, M. K.; Sarkar, A.; Narizzano, R.; Paddeu, S.; Nicolini, C. *Nanotechnology* **2000**, *11*, 30–36.
- (27) Reitzel, N.; Greve, D. R.; Kjaer, K.; Hows, P. B.; Jayaraman, M.; Savoy, S.; McCullough, R. D.; McDevitt, J. T.; Bjornholm, T. *J. Am. Chem. Soc.* **2000**, *122*, 5788–5800.
- (28) Schottland, P.; Fichet, O.; Teyssie, D.; Chevrot, C. *Synth. Met.* **1999**, *101*, 7–8.
- (29) Zhou, P. G.; Samuelson, L.; Alva, K. S.; Chen, C. C.; Blumstein, R. B.; Blumstein, A. *Macromolecules* **1997**, *30*, 1577–1581.
- (30) Paddeu, S.; Ram, M. K.; Nicolini, C. *J. Phys. Chem. B* **1997**, *101*, 4759–4766.
- (31) Granholm, P.; Paloheimo, J.; Stubb, H. *Phys. Rev. B* **1997**, *55*, 13658–13663.
- (32) Ram, M. K.; Carrara, S.; Paddeu, S.; Maccioni, E.; Nicolini, C. *Langmuir* **1997**, *13*, 2760–2765.
- (33) Kim, J.; Levitsky, I. A.; McQuade, D. T.; Swager, T. M. *J. Am. Chem. Soc.* **2002**, *124*, 7710–7718.
- (34) Ki, F.; Kwan, S.; Akana, J.; Jang, P. *J. Am. Chem. Soc.* **2001**, *123*, 4360–4361.
- (35) Li, X.; Zhang, L.; Wang, X.; Shimoyama, I.; Sun, X.; Seo, W.-S.; Dai, H. *J. Am. Chem. Soc.* **2007**, *129*, 4890–4891.
- (36) Agbor, N. E.; Petty, M. C.; Monkman, A. P. *Sens. Actuators, B* **1995**, *28*, 173–179.
- (37) Irimia-Vladu, M.; Fergus, W. J. *Synth. Met.* **2006**, *156*, 1401–1407.
- (38) Yan, X. B.; Han, Z. J.; Yang, Y.; Tay, B. K. *Sens. Actuators, B* **2007**, *123*, 107–113.
- (39) Andreu, Y.; Marcos, S.; Castillo, J. R.; Galban, J. *Talanta* **2005**, *65*, 1045–1051.
- (40) Syed, A. A.; Dinesan, M. K. *Synth. Met.* **1990**, *36*, 209–215.
- (41) Ren, J.; He, F.; Zhang, L.; Su, C.; Liu, Z. *Sens. Actuators, B* **2007**, *125*, 510–516.
- (42) Nemzer, L. R.; Schwartz, A.; Epstein, A. J. *Macromolecules* **2010**, *43*, 4324–4330.
- (43) Kausaite-Minkstiene, A.; Mazeiko, V.; Ramanaviciene, A.; Ramanavicius, A. *Sens. Actuators, B* **2011**, *158*, 278–285.
- (44) Zhang, J.; Burt, D. P.; Whitworth, A. L.; Mandler, D.; Unwin, P. R. *Phys. Chem.* **2009**, *11*, 3490–3496.
- (45) Dhanabalan, A.; Riul, A., Jr.; Mattoso, L. H. C.; Oliveira, O. N., Jr. *Langmuir* **1997**, *13*, 4882–4886.
- (46) Ram, M. K.; Bertoncello, P.; Nicolini, C. *Electroanalysis* **2001**, *13*, 574–581.
- (47) Lee, K.; Heeger, A.; Cao, Y. *Synth. Met.* **1995**, *69*, 261–262.
- (48) Bernard, M. C.; Hugot-LeGoff, A.; Joiret, S.; Arkoub, H.; Saidani, B. *Electrochim. Acta* **2005**, *50*, 1615–1623.
- (49) Louarn, G.; Lapkowski, M.; Quillard, S.; Pron, A.; Buisson, J. P.; Lefrant, S. *J. Phys. Chem.* **1996**, *100*, 6998–7006.
- (50) Cochet, M.; Louarn, G.; Quillard, S.; Buisson, J. P.; Lefrant, S. *J. Raman Spectrosc.* **2000**, *31*, 1041–1049.
- (51) Nascimento, G. M.; Silva, C. H. B.; Temperini, M. L. A. *Polym. Degrad. Stab.* **2008**, *91*, 291–297.